

Methane Reforming Process by means of a Carbonated Na₂ZrO₃ Catalyst

J. Arturo Mendoza-Nieto, Elizabeth Vera, and Heriberto Pfeiffer*

Instituto de Investigaciones en Materiales, Universidad Nacional Autónoma de México, Circuito Exterior s/n Cd. Universitaria, Del. Coyoacán, CP 04510, Ciudad de México, Mexico

(E-mail: pfeiffer@iim.unam.mx)

Sodium zirconate (Na₂ZrO₃) was synthesized by a solid-state reaction and then it was tested in the methane reforming process. Na₂ZrO₃ was initially carbonated at different temperatures (550–700 °C). Then, each carbonated Na₂ZrO₃ sample (composed by Na₂CO₃ and ZrO₂) was used as a catalyst and as a carbon dioxide supplier for syngas (H₂ + CO) production through the methane reforming reaction. Results clearly show the formation of H₂ and CO, evidencing a catalytic conversion. Moreover, cyclic and structural analyses corroborated that Na₂ZrO₃ could be used cyclically in the carbonation and subsequent methane reforming processes, although the crystalline structure was not totally recovered.

Keywords: H₂ production | Sorption-enhanced methane reforming (SEMR) | Sodium zirconate

The large increment in CO₂ emissions from fossil fuels in the last decades has become a threat to the environment. Therefore, the search for alternative and cleaner energy sources is an important scientific challenge. In this regard, H₂ production would be a viable solution for increasing energy demands.¹ Among the H₂ production processes, the most commonly used methods are steam methane reforming (SMR), water-gas shift reaction (WGSR), dry methane reforming, and ethanol-steam reforming methods.^{2–7} All of them produce syngas, composed of H₂ and CO or CO₂. Here, the removal of CO or CO₂ is usually a key step to purify H₂, and different technologies have been developed over the last years in order to accomplish it.^{8,9} Sorption-enhanced methane reforming (SEMR) can produce highly pure H₂ by using a mixture of a catalyst for the SMR and a suitable CO₂ captor.^{3,4,10} This process presents important advantages over the SMR technology (which is industrially the most used method for H₂ production), such as lower temperature operation, higher conversion yields, and the reduction of subsequent purification requirements.^{4,11}

CO₂ sorbents must satisfy some properties for being used in SEMR, for instance selective CO₂ absorption in the presence of steam, regeneration ability, good sorption–desorption kinetics, and stability under temperature and steam.^{1,11} Recently, different alkaline ceramics have been proposed as suitable CO₂ captors for the SEMR, such as CaO,¹ Na₂ZrO₃,⁵ Li₄SiO₄,^{1,12} and Li₂ZrO₃.^{3,11,12} Up to now, there are few reports in literature about methane reforming using these materials.^{3,11,13–19} In all those works, a reactor modeling of SEMR has been only theoretically proposed, suggesting the use of alkaline ceramics for CO₂ capture along with another material for methane reforming, e.g. Ni/MgO catalyst.¹³ However, these proposals present the disadvantage that H₂ production requires the use of two different materials. It must be pointed out that there is no experimental evidence of syngas production using this kind of alkaline

ceramics. Thus, the aim of this work was to study, experimentally, if Na₂ZrO₃ can be used for hydrogen production, acting first as a CO₂ captor and then as a catalytic material, during dry methane reforming process.

Sodium zirconate was synthesized by a solid-state reaction.^{16,19} Na₂CO₃ and ZrO₂ were mechanically mixed and calcined in air atmosphere at 900 °C for 12 h. A batch of Na₂ZrO₃ was tested in dry reforming reaction in a Bel-Rea catalytic reactor from Bel Japan, using 200 mg of sample. Initially, samples were carbonated dynamically from 30 °C at different temperatures (550, 600, 650, and 700 °C), using a gas mixture of 60 vol % CO₂ (Praxair, grade 3.0) and 40 vol % N₂ (Praxair grade 4.8) with a total flow rate of 100 mL min⁻¹. Later, samples were isothermally treated at the final carbonation temperature for 0.5 h and then cooled down until 200 °C using the same gas mixture. Finally, samples were dynamically heated from 200 to 900 °C with a heating rate of 2 °C min⁻¹ using 100 mL min⁻¹ of a gas mixture composed of CH₄ (5 vol %, Praxair grade 5.0) complemented with N₂. Reforming gas products were analyzed each 15 °C until 900 °C, using a Shimadzu GC 2014 gas chromatograph with a Carboxen-1000 column and an Alpha Platinum FTIR spectrometer from Bruker connected to a ZnS gas flow cell. Cyclic experiments were performed repeating the same experimental procedure described above.

Pristine Na₂ZrO₃ and reforming products were characterized by powder X-ray diffraction in the 10° ≤ 2θ ≤ 80° range, using a goniometer speed of 1°(2θ)min⁻¹, with a diffractometer Siemens D5000 coupled to a cobalt anode (λ = 1.789 Å) X-ray tube.

Figure 1 shows the CH₄ dynamic conversion to syngas evaluated after a Na₂ZrO₃ carbonation process at 600 °C. Between 200 and 750 °C, CO and H₂ production was not detected by FTIR and GC, respectively, indicating that the CH₄ reforming process was not produced in that temperature range. However, at temperatures higher than 750 °C, CO and H₂ formation became evident, fitting with the CH₄ reduction content (Figure 1A). Additionally, CO evolution was followed via FTIR analysis (Figure 1B). The CO vibration bands were identified between the 2230 and 2030 cm⁻¹ range. Also, the reactants presented vibration bands in the FTIR spectra. Methane showed signals at 1390–1170 and 3200–2600 cm⁻¹, whereas CO₂ at 725–600, 2400–2235, and 3750–3560 cm⁻¹. Figure 1C shows the hydrogen chromatograph peak, which increases between 750 and 900 °C. The highest amount of hydrogen (0.65 sccm) was obtained at 900 °C, during dry reforming process. Conversely, CO₂ was evidenced between 670 and 830 °C, which indicates that CO₂ is being desorbed from carbonated Na₂ZrO₃. The CO₂ desorption is in good agreement with the subsequent thermally CH₄ reforming process. Therefore, all these results confirm that CH₄ reforming is taking place

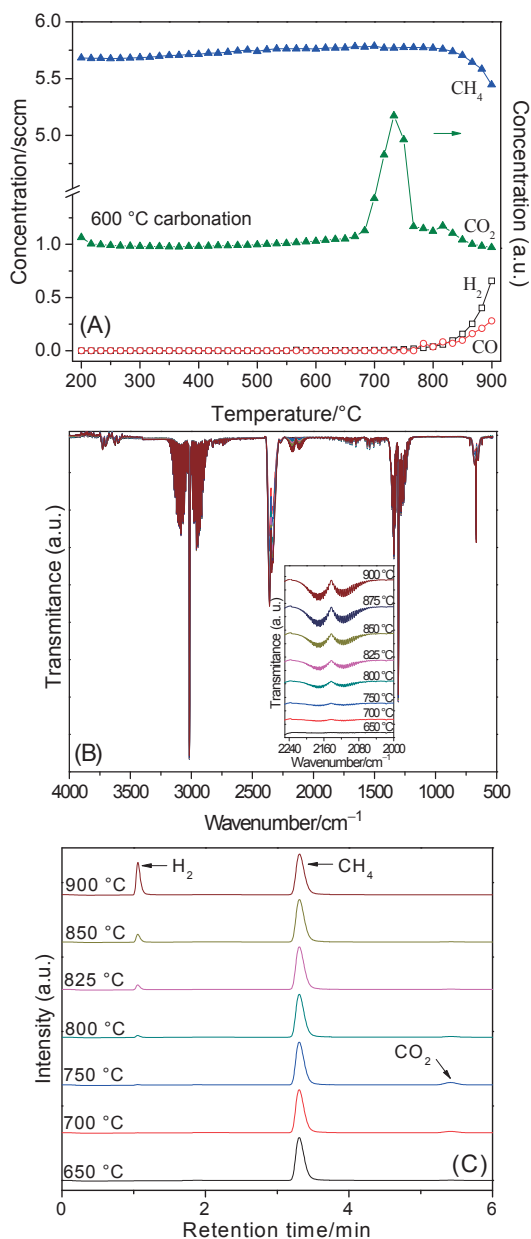
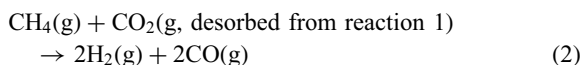
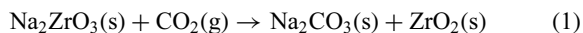


Figure 1. (A) Dynamic evolution, (B) FTIR spectra, and (C) chromatograms for methane reforming process, using Na_2ZrO_3 sample carbonated dynamically at 600 °C.

in the Na_2ZrO_3 previously carbonated particles, according to the following reaction mechanism:



A second set of experiments were performed varying the Na_2ZrO_3 carbonation temperature. In all the cases, the reforming process was produced. However, the maximum hydrogen production varied as a function of carbonation and methane reforming temperatures (Figure 2). Nevertheless, independently of the methane reforming temperature, the best hydrogen production was always obtained when the Na_2ZrO_3 carbonation

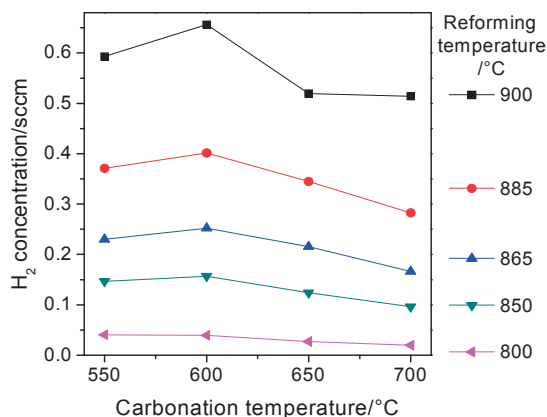


Figure 2. Thermal evolution of CH_4 reforming from 800 to 900 °C using Na_2ZrO_3 samples carbonated dynamically at different final temperatures (550, 600, 650, and 700 °C).

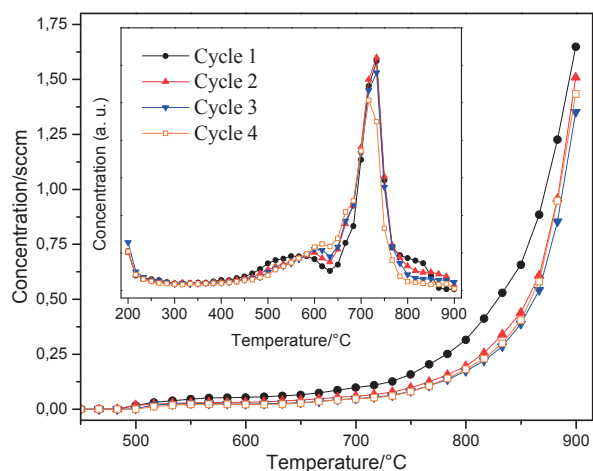


Figure 3. Dynamic evolution for hydrogen and carbon dioxide (inset) gases during the methane reforming process, into cyclic processes.

temperature was 600 °C. It may be related to the $\text{Na}_2\text{CO}_3\text{-ZrO}_2$ external shell microstructural properties. It has been reported that Na_2ZrO_3 carbonation produces different $\text{Na}_2\text{CO}_3\text{-ZrO}_2$ external shell microstructures, depending on the temperature.¹⁶ At $T \leq 550$ °C the external shell is composed by a mesoporous shell, which improves different diffusion processes. It must be pointed out that in the present work, the CO_2 flow used for the carbonation process was different (see the experimental section), which must have modified the temperature limit for mesoporous formation. Based on the results shown in Figure 2, it seems that higher Na_2ZrO_3 carbonation temperatures may have densified the $\text{Na}_2\text{CO}_3\text{-ZrO}_2$ external shell, reducing CO_2 desorption, and consequently, the methane reforming process.

In order to analyze the possible cyclability of Na_2ZrO_3 in carbonation and subsequent CH_4 dynamic conversion to syngas, four cycles were performed into the same experimental conditions described above using a new Na_2ZrO_3 batch. Figure 3 shows the hydrogen and carbon dioxide gas chromatograph peaks' evolution during the methane reforming process.

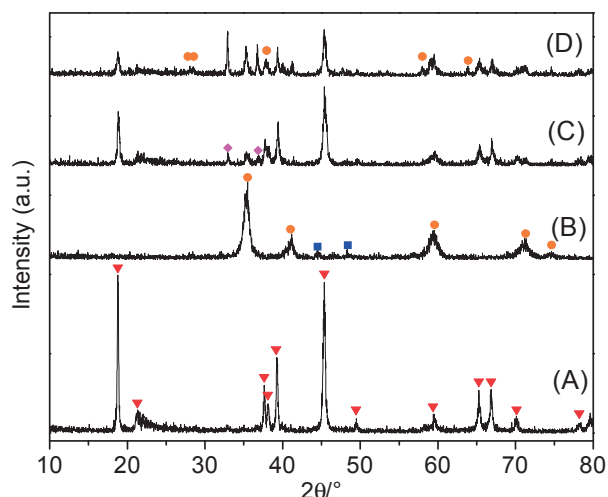


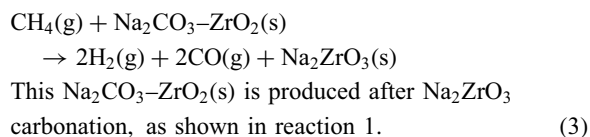
Figure 4. XRD patterns of (A) original material, (B) dynamically carbonated Na_2ZrO_3 , (C) material obtained after CH_4 reforming, and (D) material obtained after four CH_4 reforming processes. Crystalline phases of (∇) Na_2ZrO_3 , (\square) Na_2CO_3 , (\circ) monoclinic ZrO_2 , and (\diamond) tetragonal ZrO_2 .

Hydrogen was produced between 750 and 900 °C for all the cycles, where the highest hydrogen amounts decreases from 1.65 to 1.43 sccm in the first and fourth cycles, respectively. It corresponds to a 13.3% decrement in the hydrogen production, although it should be pointed out that the main decrement is produced between the first two cycles. Latter cycles seem to stabilize.

In addition, the square inset of Figure 3 shows CO_2 evolution, produced during the Na_2ZrO_3 decarbonation process. As it can be seen, Na_2ZrO_3 decarbonation does not present any important variation among cycles, indicating that the initial step of the whole process (Na_2ZrO_3 carbonation–decarbonation) is not importantly affected by the catalytic methane reforming process.

During the CO_2 desorption process, it should be analyzed if sodium zirconate was able to be regenerated. Based on that, different sample products were analyzed by X-ray diffraction (XRD). Figure 4 shows the pristine Na_2ZrO_3 used for the different experiments, where no other crystalline phases were detected. In this case, the Na_2ZrO_3 sample was fitted to the JCPDS card 35-0770, which corresponds to a monoclinic crystalline structure. When Na_2ZrO_3 was carbonated at 600 °C, the XRD pattern showed the formation of Na_2CO_3 (JCPDS card 37-0451) and ZrO_2 (JCPDS card 36-0420), according to reaction 1. The different diffraction peak intensities, observed between ZrO_2 and Na_2CO_3 phases, corresponds to Zr and Na diffraction scattering coefficients differences. Finally, the XRD pattern of the sample products after one or four methane reforming cycles showed the presence of Na_2ZrO_3 as the main phase, as well as different ZrO_2 phases (tetragonal and monoclinic) as minor secondary phases. The presence of tetragonal and monoclinic ZrO_2 indicates that part of the sodium content has been lost during cycles, perhaps through a sublimation process. In the tetragonal ZrO_2 case, it may be produced by a Na-doped ZrO_2 structure.¹⁷

Summarizing, the results confirmed that Na_2ZrO_3 is able to capture CO_2 (as it was already published^{16–18}) and subsequently perform the corresponding reforming process. The catalytic process is produced in the presence of methane through a simultaneous CO_2 desorption. This process can be produced cyclically, where the Na_2ZrO_3 structure is highly regenerated after the double carbonation–catalytic process. Based on these results, reaction 2 would be modified as follows:



This work was financially supported by the projects SENER-CONACYT and PAPIIT-UNAM. E. Vera and J. A. Mendoza-Nieto thank to CONACYT and DGAPA-UNAM for financial support, respectively. Finally, authors thank to A. Tejada for technical help.

References and Notes

- 1 Y. Chen, Y. Zhao, J. Zhang, C. Zheng, *Sci. China: Technol. Sci.* **2011**, *54*, 2999.
- 2 A. F. Lucrédio, E. M. Assaf, *J. Power Sources* **2006**, *159*, 667.
- 3 M. H. Halabi, M. H. J. M. de Croon, J. van der Schaaf, P. D. Cobden, J. C. Schouten, *Chem. Eng. J.* **2011**, *168*, 872.
- 4 J. R. Hufton, S. Mayorga, S. Sircar, *AIChE J.* **1999**, *45*, 248.
- 5 A. L. Ortiz, M. A. E. Bretado, J. S. Gutiérrez, M. M. Zaragoza, R. H. L. Castro, V. C. Martínez, *Int. J. Hydrogen Energy* **2015**, *40*, 17192.
- 6 D. Y. A. Olivas, M. R. B. Guerrero, M. A. E. Bretado, M. M. da Silva Paula, J. S. Gutiérrez, V. G. Velderrain, A. L. Ortiz, V. Collins-Martínez, *Int. J. Hydrogen Energy* **2014**, *39*, 16595.
- 7 K. Essaki, T. Muramatsu, M. Kato, *Int. J. Hydrogen Energy* **2008**, *33*, 6612.
- 8 S. D. Kenarsari, D. Yang, G. Jiang, S. Zhang, J. Wang, A. G. Russell, Q. Wei, M. Fan, *RSC Adv.* **2013**, *3*, 22739.
- 9 B. Alcántar-Vázquez, E. Vera, F. Buitron-Cabrera, H. A. Lara-García, H. Pfeiffer, *Chem. Lett.* **2015**, *44*, 480.
- 10 M. S. Yancheshmeh, H. R. Radfarnia, M. C. Iliuta, *Chem. Eng. J.* **2016**, *283*, 420.
- 11 E. Ochoa-Fernández, H. K. Rusten, H. A. Jakobsen, M. Rønning, A. Holmen, D. Chen, *Catal. Today* **2005**, *106*, 41.
- 12 H. K. Rusten, E. Ochoa-Fernández, H. Lindborg, D. Chen, H. A. Jakobsen, *Ind. Eng. Chem. Res.* **2007**, *46*, 8729.
- 13 M. H. Halabi, M. H. J. M. de Croon, J. van der Schaaf, P. D. Cobden, J. C. Schouten, *Chem. Eng. J.* **2011**, *168*, 883.
- 14 J. P. Jakobsen, E. Halmøy, *Energy Procedia* **2009**, *1*, 725.
- 15 E. Ochoa-Fernández, G. Haugen, T. Zhao, M. Rønning, I. Aartun, B. Børresen, E. Rytter, M. Rønnekleiv, D. Chen, *Green Chem.* **2007**, *9*, 654.
- 16 L. Martínez-dlCruz, H. Pfeiffer, *J. Phys. Chem. C* **2012**, *116*, 9675.
- 17 L. Martínez-dlCruz, H. Pfeiffer, *J. Solid State Chem.* **2013**, *204*, 298.
- 18 I. Alcérrecá-Corte, E. Fregoso-Israel, H. Pfeiffer, *J. Phys. Chem. C* **2008**, *112*, 6520.
- 19 G. G. Santillán-Reyes, H. Pfeiffer, *Int. J. Greenhouse Gas Control* **2011**, *5*, 1624.